Available online at www.sciencedirect.com
ScienceDirect
Journal of the European Ceramic Society 27 (2007) 2171–2181
www.elsevier.com/locate/jeurceramsoc

High-temperature hot-pressing of titanium carbide–graphite hetero-modulus ceramics

Igor L. Shabalin [a,*], David M. Tomkinson [a], Leonid I. Shabalin [b]

[a] *Institute for Materials Research, The University of Salford, Greater Manchester M5 4WT, UK*
[b] *Russian State Professional and Pedagogical University, Yekaterinburg 620012, Russia*

Received 7 April 2006; received in revised form 12 July 2006; accepted 15 July 2006
Available online 7 September 2006

Abstract

Hetero-modulus ceramic–ceramic composite materials (HMC) present the combination of ceramic matrix with high Young's modulus and the inclusions of a dispersed phase with low Young's modulus. The densification of 60–100 vol% TiC–0–40 vol% C (graphite) HMC during hot-pressing of powder compositions at 2200–2400 °C and applied pressures of 8–16 MPa is studied. The general theory of bulk-viscous flow for porous body is developed to describe obtained experimental data. This relation as well as Kovalchenko's equation for the evolution of relative density for non-uniform deformation of porous body, incorporating different stages of creep, are used to determine the activation energy and the exponent constant of hot-pressing process, which values are 270 ± 30 kJ mol^{-1} and 3 ± 0.3, respectively. The obtained experimental data are discussed on the basis of extensive and detailed analysis of the previous studies on diffusion and diffusion-related phenomena in the Ti–C system.

Keywords: Hot-pressing; Composites; Carbides; Carbon; Hetero-modulus ceramics

1. Introduction

Hetero-modulus ceramic–ceramic composite materials (HMC) present the combination of ceramic matrix with high Young's modulus (300–600 GPa) and the inclusions of a dispersed phase with significantly lower Young's modulus (15–20 GPa). By means of the making of HMC, it becomes possible to use brittle refractory compounds (carbides, nitrides, borides, silicides, oxides) in the most modern high-temperature structures. The generally low thermal shock resistance of these materials with the highest elastic modulus can be greatly improved by the addition of low-modulus graphite and graphite-like boron nitride inclusions.[1] Another great advantage of HMC is an excellent machinability by conventional tools with a high grade of accuracy[2] that is normally impossible with conventional ceramics.

Refractory carbide–carbon composites[3] are prospective materials for high-temperature application, e.g. as thermally stressed parts of rocket engines, elements of thermal protection for re-entry flying apparatus, highly loaded brake-shoes in aviation and automotive engineering, high-temperature heating elements and others, including titanium carbide–graphite composition, which above all, because of its relatively low Z, is a candidate for thermonuclear and fusion reactors as a plasma facing material.[4]

High-temperature hot-pressing technique possesses practically unlimited possibilities for the production of HMC based on different high-modulus matrices and low-modulus additives in the widest range of their content ratios. But, though the densification during hot-pressing for refractory carbides and their powder compositions with metals were studied thoroughly,[5–8] no kinetics data on carbide–carbon compositions densified by similar processes have been yet published.

Therefore, the goal of the present work is to study the kinetics and mechanism of densification for titanium carbide–graphite compositions as a general example of hot-pressing processing for HMC fabrication, to find an acceptable description of the process, which could be used for the subsequent modeling of evolution for porous structures in refractory carbide–carbon systems, and to compare with those inherent to single phase metal carbides.

* Corresponding author. Tel.: +44 161 295 3269; fax: +44 161 295 5147.
E-mail address: i.shabalin@salford.ac.uk (I.L. Shabalin).

0955-2219/$ – see front matter © 2006 Elsevier Ltd. All rights reserved.
doi:10.1016/j.jeurceramsoc.2006.07.008

2. Experimental procedure

The matrix for the HMC in the present investigation of high-temperature hot-pressing densification kinetics consisted of carbothermic titanium carbide powders (KZTS, Sverdlovsk Region, Russia) equiaxed but irregular in shape with a particle size 1–4 μm, contained 78.5 wt.% Ti, 19.6 wt.% C, 0.7 wt.% W, 0.5 wt.% O, 0.4 wt.% Fe, 0.1 wt.% Co. The powders of natural graphite marked YeUZ-M and standardized by GOST 10274-82 (KKZ, Chelyabinsk Region, Russia) with mineral remains less than 0.1 wt.% were used as low-modulus additives. The densities d determined by XRD method were 4.90 and 2.26 g cm^{-3} for titanium carbide and graphite phases, respectively. The compositions were prepared by mixing in a rolling mill with rubber-coated milling rods. Hot-pressing was conducted in a set of dies made of structural graphite marked GMZ-A (ChYeZ, Chelyabinsk, Russia) of 70 mm outside diameter and 20 mm inside diameter. Approximately 15 g of dried 60–100 vol% TiC–0–40 vol% C powder compositions was charged into graphite die set for each hot-pressing run.

A technological map of hot-pressing processing together with a typical curve of measured linear shrinkage of a specimen is shown in Fig. 1. The general parameters of hot-pressing process, temperature T and applied pressure P, were changed in the ranges as follows: 2200–2400 °C and 8–16 MPa, respectively, at that time the furnace pressure in each of the experiments was fixed at two levels: 1 Pa (the pressure of residual gases) – before the isothermal mode (soaking) was achieved and 20 kPa (the pressure of argon atmosphere) – after its beginning. The values of parameters T and P were chosen on the grounds of the practice of HMC production by hot-pressing.

Dilatometric measurements of a specimen height h were carried out permanently by means of a special mechanical sensor with a 2.5 μm-accuracy. Special experiments were used to determine the thermal drift of the dilatometric measuring system. The apparent density of polished hot-pressed specimens calculated after the procedures of machining, weighing and linear measuring was used to determine the final relative density γ_f according to equation:

$$\gamma_f = \frac{d}{v_{TiC}d_{TiC} + v_C d_C} \times 100\% \quad (1)$$

where d is the apparent density of hot-pressed titanium carbide—graphite HMC specimen, v_{TiC}, v_C, respectively, the titanium carbide and graphite contents in composition, vol%, and d_{TiC}, d_C, respectively, the titanium carbide and graphite XRD densities, g cm^{-3}. The relative density γ at any time τ during the hot-pressing with constant pressure under isothermal conditions was calculated from the data on the linear shrinkage[9]:

$$\gamma = \gamma_f \left(\frac{h_f}{h}\right) \quad (2)$$

where h_f is the final height of a hot-pressed specimen measured by the dilatometric system and h the current height of the specimen during the hot-pressing processing, so a hot-pressing densification kinetic curve was established from the calculated values.

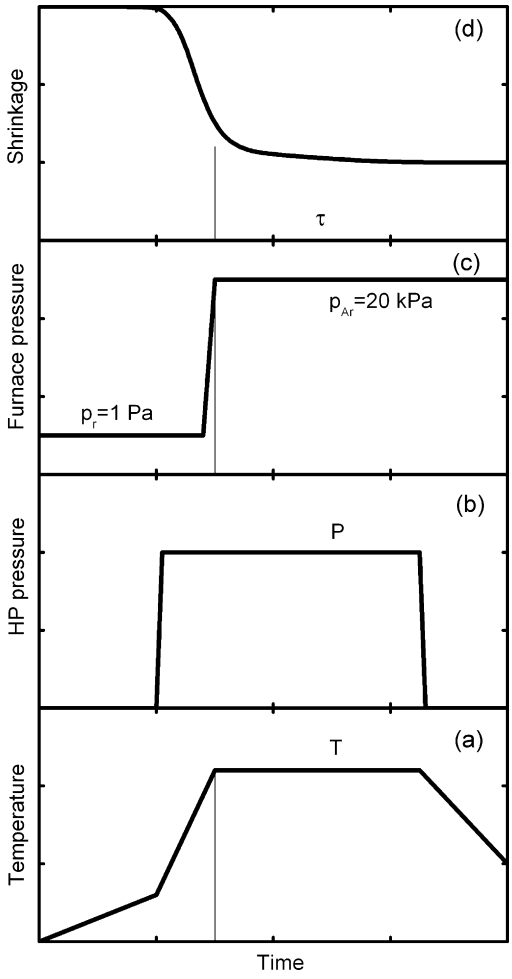

Fig. 1. Technological map for investigation of the densification kinetics as evolutions of temperature T (a), applied pressure P (b) and furnace pressure (atmosphere) p_n (c) with hot-pressing processing time t combined with a typical dilatometric curve of measured linear shrinkage (d) for a TiC–C HMC specimen.

The elicitation of the interface boundaries while microstructure researching was provided by anode etching of the polished specimens of the hot-pressed TiC–C HMC in the sodium–phosphate electrolyte with the addition of the catalytic $CuSO_4$–H_2SO_4 solution[10]. The anodization of specimens was conducted under voltage 3.5 V for 20–30 s at room temperature. The colored microstructure of the compositions were observed in Epitype-2 (Carl Zeiss Jena, Germany) optical microscope and photographed with micro-photo equipmen MFN-12 (LOMO, Russia).

3. Results and discussion

3.1. Densification kinetics

The total shrinkage of TiC–C HMC during the complete cycle of high-temperature hot-pressing given by

$$S = \left(\frac{\Delta h}{h}\right)_t = \frac{h_{cp} - h_f}{h_{cp}} \times 100\% \quad (3)$$

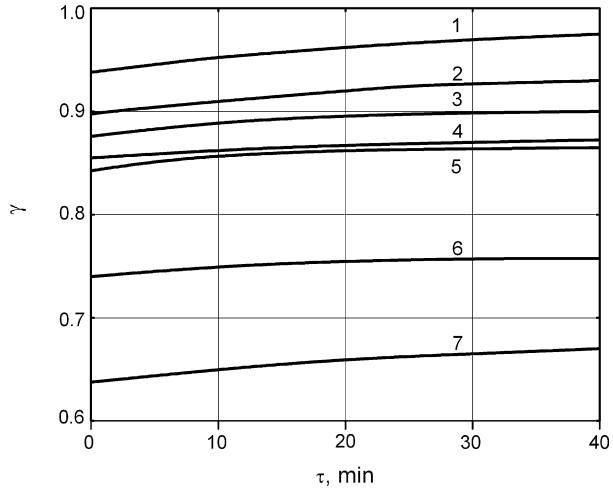

Fig. 2. Evolutions of the relative density γ for 80 vol% TiC–20 vol% C composition with isothermal soaking time τ during hot-pressing processing at different temperatures: (2, 5, 7) $T = 2200\,^{\circ}$C; (1, 4, 6) $T = 2300\,^{\circ}$C; (3) $T = 2400\,^{\circ}$C and applied pressures: (6 and 7) $P = 8$ MPa; (3–5) $P = 12$ MPa; (1 and 2) $P = 16$ MPa.

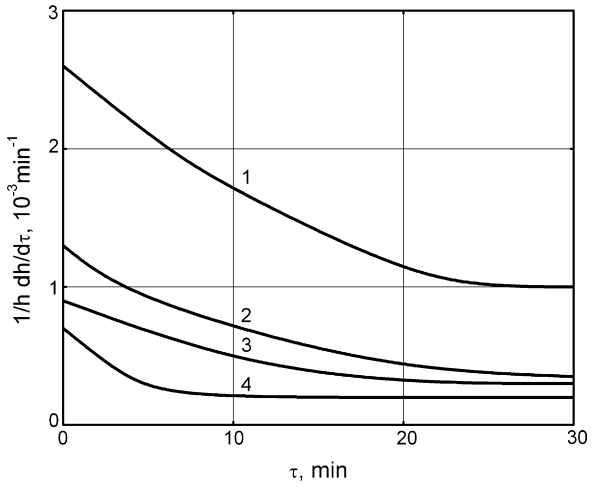

Fig. 3. Evolutions of the shrinkage rate $1/h \times \mathrm{d}h/\mathrm{d}\tau$ for 80 vol% TiC–20 vol% C composition with isothermic soaking time τ during hot-pressing processing at different temperatures: (2) $T = 2300\,^{\circ}$C; (1, 3, 4) $T = 2400\,^{\circ}$C and applied pressures: (2 and 4) $P = 8$ MPa; (3) $P = 12$ MPa; (1) $P = 16$ MPa.

where h_{cp} is the height of the cold-pressed specimen before hot-pressing processing, amounted to 30–80% dependent on carbide–carbon ratio in HMC (see Fig. 1d). The total shrinkage S considerably increased with other equal parameters, when the volume percentage of low-modulus graphite additive rises. The numerous experiments of TiC–C hot-pressing processing showed that shrinkage of HMC and densification corresponding to it mostly were observed during the heating of materials up to the temperature of isothermal soaking T, so the increase of density on the stage with the constant values of parameters T and P occured in rather limited terms.

The evolutions of relative density γ while hot-pressing for the 80 vol% TiC–20 vol% C HMC are presented in Fig. 2. The increase of temperature T and pressure P significantly caused the density of HMC that was reached during the hot-pressing isothermal soaking under the constant applied pressure. The rate of linear shrinkage during the isothermal soaking reduced from the highest to a practically constant lower value for fixed T and P (Fig. 3). This transition to the constant value was passed as soon as higher temperature and lower pressure of the soaking. The enlargement of the soaking time higher than 30–40 min was insignificant for the final density of hot-pressed material.

The theory of bulk-viscous flow for porous body,[11] based on the general theory of deformation of solids, gives us for the case of uniaxial compression with the absence of transversal strains the expression for the relative density as follows:

$$\frac{\mathrm{d}\gamma}{\mathrm{d}\tau} = -\frac{3P(1-\gamma)}{4\eta\gamma} \tag{4}$$

where η is the coefficient of shear viscosity for porous body. The integration of Eq. (4) leads to:

$$\ln\frac{\gamma_0 - 1}{\gamma - 1} - (\gamma - \gamma_0) = \frac{3P}{4}\int_0^{\tau}\frac{\mathrm{d}\tau}{\eta} \tag{5}$$

In the earlier papers devoted to the hot-pressing processing of single phase carbide materials[5–7] it was shown that the value of coefficient of shear viscosity for porous carbides while being densified increases, and thus, it is a variable dependant on time of treatment.

The densification process of the TiC–C HMC considerably differs from those for pure carbides, because of constant value for coefficient of shear viscosity during the isothermal soaking. That is expressed by linear dependence on time for the value of $\Phi(\gamma) = \ln(1-\gamma) - (1-\gamma)$, which is supposed in the case of the integration of Eq. (4) taking into account the independent character of η:

$$\ln(1-\gamma) - (1-\gamma) = -\frac{3P}{4\eta}\tau + \ln(1-\gamma_0) - (1-\gamma_0) \tag{6}$$

or

$$\Phi(\gamma) - \Phi(\gamma_0) = -\frac{3P}{4\eta}\tau \tag{7}$$

$$\Delta\Phi(\gamma) = -\frac{3P}{4\eta}\tau \tag{8}$$

At the same time in similar conditions of the hot-pressing, the coefficient of shear viscosity for 100 vol% TiC composition appeared to be a time-dependant parameter (Fig. 4).

The increase of carbon volume content v_C in the hot-pressed TiC–C HMC caused the corresponding decrease of the final relative density γ_f and increase of viscosity (slope of lines in the plots of $\Phi(\gamma) - \tau$) during the procedure.

3.2. Influence of temperature and applied pressure

The growth of viscosity is observed also while values of temperature T and pressure P, parameters of hot-pressing process, are reduced. The examples of dependencies $\Phi(\gamma) - \tau$ for 80 vol% TiC–20 vol% C are shown in Fig. 5. All those experimental dependencies are characterized by constant values for the coefficient of shear viscosity during the hot-pressing, which could be calculated accordingly to Eqs. (6)–(8) for the

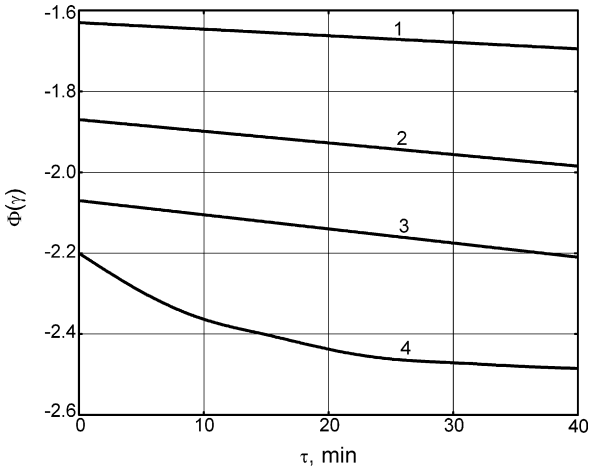

Fig. 4. Characteristics of densification $\Phi(\gamma)$ during hot-pressing processing for the TiC–C compositions at $T = 2300\,^{\circ}C$ and $P = 12$ MPa: 1–60 vol% TiC–40 vol% C; 2–70 vol% TiC–30 vol% C; 3–80 vol% TiC–20 vol% C; 4–100 vol% TiC.

different experimental temperatures T and pressures P. For 80 vol% TiC–20 vol% C composition the values of η lie in $(0.3–3.0) \times 10^{11}$ Pa s interval, that is one order of magnitude higher than Kovalchenko[12] had obtained for the single phase TiC hot-pressed at the similar temperatures and pressures.

Linearization of the coefficient of viscosity dependency on temperature in the coordinates of $\ln(\eta/T) - 1/T$ (Fig. 6) allows to determine the activation energy of viscous flow Q in accordance to the mechanics of continuum media equation[13]:

$$\eta = A'T \exp\left(\frac{Q}{RT}\right) \tag{9}$$

where A' is a constant independent on temperature, having dimension of kg m^{-1} s^{-1} K^{-1}.

Application of this equation for studied hot-pressing processes gave for the activation energy Q a value of 270 ± 30 kJ mol^{-1}.

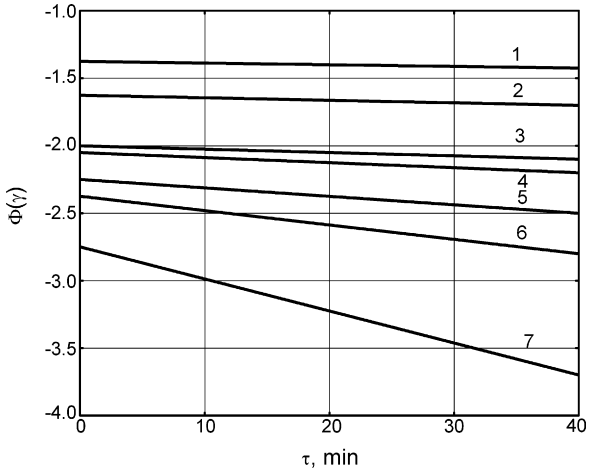

Fig. 5. Characteristics of densification $\Phi(\gamma)$ during hot-pressing processing for 80 vol% TiC–20 vol% C composition at different temperatures: (1, 3, 6) $T = 2200\,^{\circ}C$; (2, 4, 7) $T = 2300\,^{\circ}C$; (5) $T = 2400\,^{\circ}C$ and applied pressures: (1 and 2) $P = 8$ MPa; (3–5) $P = 12$ MPa; (6 and 7) $P = 16$ MPa.

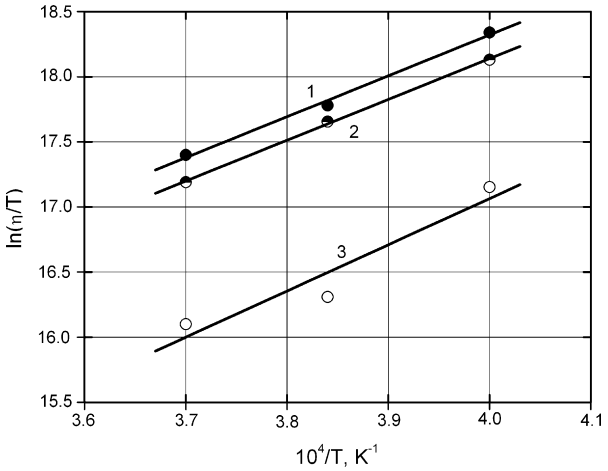

Fig. 6. The Arrenius plot of $\ln(\eta/T)$ for the hot-pressed 80 vol% TiC—20 vol% C composition at different applied pressures, P: (1) 8 MPa; (2) 12 MPa; (3) 16 MPa.

Analysis of obtained experimental data for the viscosity dependency on applied pressure during hot-pressing in $\lg\eta - \lg P$ coordinates (Fig. 7) leads to:

$$\eta = A'' P^{-k} \tag{10}$$

where A'' is a constant independent on applied pressure. Eq. (10) is similar to the equation proposed by Skorokhod[11] for the effective non-elastic viscosity describing the rheological particularities of non-linear creep of porous body. The obtained experimental data give us a value for k of 3 ± 0.3. By combining Eqs. (9) and (10), it is possible to submit the generalized expression for the coefficient of shear viscosity for porous matter during hot-pressing:

$$\eta = \mathrm{ATP}^{-k} \exp\left(\frac{Q}{RT}\right) \tag{11}$$

where A is a constant independent on the T and P parameters. The constant A reflects the capability of the microstructure of porous system to densify (sinter) while hot-pressing processing, so it

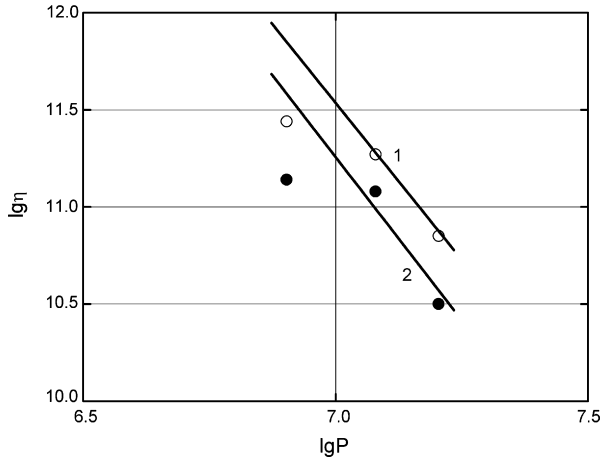

Fig. 7. The coefficient of shear viscosity values for the hot-pressed 80 vol% TiC–20 vol% C composition at different temperatures, T: (1) 2200 °C; (2) 2300 °C.

could be applied as a criterion for the preliminary preparation (e.g. milling) and content optimization (e.g. volume fraction of low-modulus additives) of HMC compositions before the high-temperature treatment.

3.3. Creep model

Inserting the generalized expression for the viscosity of porous matter that was obtained above to Eq. (7), it is possible to transform the latter one to:

$$\Phi(\gamma) - \Phi(\gamma_0) = -\frac{3}{4}\frac{1}{A}P^{k+1}\frac{1}{T}\tau \exp\left(-\frac{Q}{RT}\right) \quad (12)$$

or

$$\Delta\Phi(\gamma) = \frac{C' P^q}{RT}\tau \exp\left(-\frac{Q}{RT}\right) \quad (13)$$

Eq. (13) corresponds to a general relationship of steady-state (secondary) creep of materials[14]:

$$\dot{\varepsilon} = C\sigma^n \frac{1}{kT} \exp\left(-\frac{Q'}{kT}\right) \quad (14)$$

where $\dot{\varepsilon}$ is the strain rate during steady-state stage of creep, σ the applied stress, k the Boltzman constant, Q' the activation energy for creep, C the constant independent of applied stress σ and temperature T and n is the creep exponent constant. At high temperatures the creep exponent $n = (\partial \ln\dot{\varepsilon}/\partial \ln\sigma)_T$, which illustrates the stress sensitivity of a material,[15] could have a value from 1 to 10. When it is usually realized between 3 and 5.5 this regime is called power-law creep,[16] but in the case of the experimental evidence that $n = 1$ Eq. (14) describes a Newtonian dislocation (linear) creep as known as Harper–Dorn mechanism[14,16].

Constructing the deformation-mechanism map for the transition-metal carbides Frost and Ashby[16] applied for the TiC power-law creep exponent n the value equals 5.0, but there are contradictory data in literature. Williams[17] defined for single crystal of $TiC_{0.96}$ under compressive stress $n = 5.5$ in a temperature range of 800–1600 °C, while Spivak et al.[18,19] found for $TiC_{0.95}$ the value $n = 1$ at 2100–2300 °C, which increases to $n = 3$–4 at 2300–2600 °C. The latest study by Tsurekawa et al.[20] brought the following results for steady state strain rate: $n \approx 7$ in a temperature range of 1475–1855 °C and about 5 at 2000 °C.

From the detailed consideration of the interconnection of equations for densification during hot-pressing and creep of solid matter jointly with the general theory of volume viscous flow, Kovalchenko[21] has proposed the equation for evolution of relative density γ incorporating α-, β- and κ-creep equations for non-uniform deformation of porous body, which is realized into a rigid die while hot-pressing processing[22,23]:

$$\Delta X_n(\gamma) = \int_{\gamma_0}^{\gamma} \gamma^{(5n'+1)/2}(1-\gamma)^{-(n'+1)/2}\mathrm{d}\gamma = A(P + P_L)^{n'}\tau \quad (15)$$

where $\Delta X_n(\gamma) = X_n(\gamma) - X_n(\gamma_0)$ is a residual of antiderivative functions taken for current and initial values of relative density γ, P_L the Laplace's (capillary forces) pressure, A and n' are constants corresponding to Eq. (14): $A = C/kT$ and $n' = n$. The adequacy of this mathematical model for description of hot-pressing processes for the powders of refractory compounds was confirmed by a series of papers[21–27] (Table 1). Denisenko and Mai[28] also came to the derivation of the equation that insignificantly differs from the Kovalchenko's formula:

$$\Delta F(\gamma) = \int_{\gamma_0}^{\gamma} \gamma^{(3n''-1)/2}(1-\gamma)^{-(n''+1)/2}\mathrm{d}\gamma = MP^{n''}\tau \exp\left(-\frac{Q''}{RT}\right) \quad (16)$$

Table 1
Values of exponent constant n from Eq. (15) for different compositions based on refractory compounds

Class	Composition	n	Reference
Carbide	TiC	3	21,22
	ZrC	3	23
Nitride	TiN	3	24
Boride	TiB_2[a]	4	25
	TiB_2	3	25
	ZrB_2	2	24
	CrB_2	2	24
Silicide	$MoSi_2$	2	24
Cermet	TiC–Nb	2	26
	WC–Nb	2	26
	TiC–Ni–Mo	1	27

[a] Containing 1.5 wt.% Fe.

Application of Kovalchenko's formula for the experimental data obtained in the present work showed that Eq. (15) delineates well the densification processes of the TiC–C HMC during hot-pressing with applied constant pressure under isothermal conditions, when the value of exponent constant n equals 3. Previously the value $n = 3$ was successfully used for the model of hot-pressing processes for pure and iron-contaminated titanium carbide[21,22]. For the case with $n = 3$ Eq. (15) transformed as

$$X_3(\gamma) = \frac{\gamma^7}{7} + \frac{\gamma^6}{3} + \frac{3}{5}\gamma^5 + \gamma^4 + \frac{5}{3}\gamma^3 + 3\gamma^2 + 7\gamma + \frac{1}{1-\gamma} + 8\ln(1-\gamma) \quad (17)$$

The experimental TiC–C composition densification dependencies on time were converted with the application of tabled values of $X_3(\gamma)$ function submitted in appendix to Kovalchenko's study[22]. Those for the 80 vol% TiC–20 vol% C HMC are shown in Fig. 8. The calculated values of $X_3(\gamma)$ dependencies considered by the $\ln[T\dot{X}_3(\gamma)/(P + P_L)^3] - 1/T$ plot give us the same value for $Q = 270 \pm 30$ kJ mol^{-1}, as it was obtained previously while modeling the viscous flow processes during the hot-pressing procedure.

3.4. Recrystallization effect

Due to Arrhenius plots the analysis of thermally activated processes allows to draw several conclusions concerning the probable physical mechanism. The calculated and experimen-

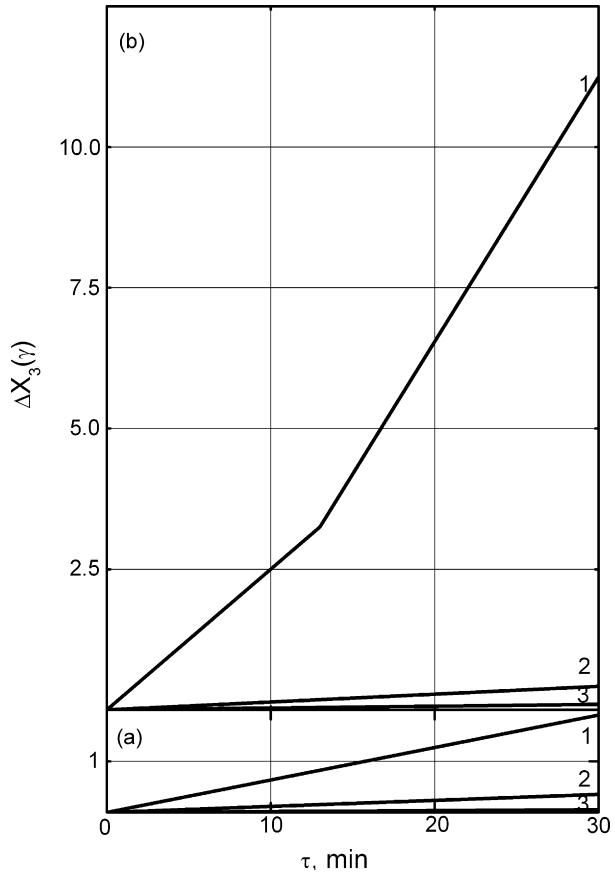

Fig. 8. Characteristics of densification $\Delta X_3(\gamma)$ during hot-pressing processing for 80 vol% TiC–20 vol% C composition at different temperatures, T: (a) 2200 °C; (b) 2300 °C and applied pressures, P: (1) 16 MPa; (2) 12 MPa; (3) 8 MPa.

tal literature data on vacancies formation and motion, diffusion and diffusion-controlled processes for the Ti–C and relative systems are shown in Tables 2–4. The values of apparent activation energy Q for titanium and carbon self-diffusion, recrystallization of carbide phase and creep behavior of the TiC compositions are collected there from different sources.

The formal kinetics analysis of densification (sintering) process for the TiC–C HMC carried out in the present work determined the direct functional relation between internal properties of treated material system (h, γ) and external parameters of influence on the system by high-temperature treatment (T, P, τ). But there is an obvious necessity to use the exploration of composite microstructure for better understanding of the physical nature of densification process, because apart from the discharge of the powder (porous) system from non-equilibrium macrodefects, i.e. sintering process, the several processes, including heterodiffusion and recrystallization, are realized during hot-pressing. In similar systems, those processes closely connect with the densification of porous matter. Micrographs of the hot-pressed TiC–C HMC with different contents of low-modulus graphite inclusions are shown in Fig. 9. The microstructure analysis of compositions revealed the significant influence of the inclusions located predominantly at the carbide grain boundaries on the matrix grain growth. The increase of graphite content from 10 to 40 vol% caused to the reduction of TiC mean grain size on 3–4 times (Fig. 10). The saturated by carbon carbide phase in HMC is characterized by the lower values of lattice parameter ($a = 0.4326$ nm) and microhardness (HV = 24 GPa) compared with those for quasi-stoichiometric TiC_{1-x}[19]. The kinetics analysis of the TiC–C HMC formation during hot-pressing undoubtedly evidences that the densification of materials is controlled by power-law creep process characterized by $\dot{\varepsilon} \propto \sigma^3$. The thermally activated glide-controlled creep with lower value of activation energy Q and exponent $n \approx 3$ is often observed during the high-temperature ceramics processing[16]. However, during the initial stages, the reaggregation of powder particles due to the interre-

Table 2
Values of the formation and motion energy E for vacancies in titanium carbide phase

Process	Phase	Energy E (kJ mol^{-1})	Reference
Formation of Ti-vacancies	$TiC_{1.0}$	345	29
Formation of C-vacancies	$TiC_{1.0}$	119	29
Formation of C-vacancies	$TiC_{0.99}$	134 ± 3	30
Motion of Ti-vacancies	$TiC_{1.0}$	300	29
Motion of C-vacancies	$TiC_{1.0}$	475	29
Motion of C-vacancies	$TiC_{0.94}$	460 ± 50	31
Motion of C-vacancies	$TiC_{1.0}$	370 ± 10	32

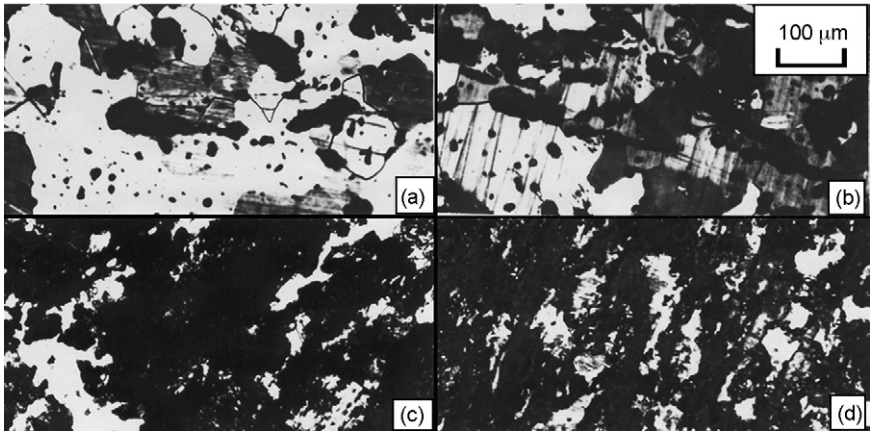

Fig. 9. Microstructures of the TiC–C hot-pressed compositions with different carbon contents: (a) 10 vol%; (b) 20 vol%; (c) 30 vol%; (d) 40 vol%, colored anode etching.

Table 3
Values of apparent activation energy Q for different types of diffusion and diffusion-controlled processes in titanium carbide

Process	Phase	Temperature range (°C)	Activation energy Q (kJ mol^{-1})	Reference
Lattice self-diffusion of Ti	$TiC_{0.67–0.97}$	1920–2215	740 ± 15	33
Lattice self-diffusion of C	$TiC_{0.97}$	1450–2280	400 ± 5	34
Lattice self-diffusion of C	$TiC_{0.84}$	2000	410	35
Grain-boundary diffusivity	TiC_{1-x}	>1800	240	36
Grain-boundary diffusivity	TiC_{1-x}	920–1645	270	37
Grain-boundary diffusivity	$TiC_{0.97}$	–	543	16
Dislocation core diffusion	$TiC_{0.97}$	–	543	16
Recrystallization[a]	TiC_{1-x}	<2000	120	38
Recrystallization[b]	$TiC_{0.98}$	1500–2050	140 ± 10	39
Recrystallization[c]	$TiC_{0.96}$	1600–2000	190	40
Recrystallization[d]	$TiC_{0.63–0.75}$	1200–1600	230 ± 5–10%	41
Recrystallization[c]	$TiC_{0.93}$	1400–2100	243 ± 6	42
Recrystallization[e]	$TiC_{0.63–0.75}$	1650–1850	260 ± 5%	43
Recrystallization[f]	$TiC_{0.93}$	2300–2500	280 ± 10	7
Creep (compression, 3.9630×10^{-5} s^{-1}, $n = 10$)	$TiC_{0.95}$	1010–1240	240 ± 10	44
Creep (compression, $3.9–630 \times 10^{-5}$ s^{-1}, $n = 5.3$)	$TiC_{0.95}$	1570–2000	470 ± 30	44
Creep (compression, 8–70 MPa, $n = 5.5$)	$TiC_{0.96}$	800–1600	320	17
Creep (compression, load relaxation)	$TiC_{0.93}$	1200–1600	390	45
Creep (compression, $2–500 \times 10^{-5}$ s^{-1}, $n = 7$)	TiC_{1-x}	1475–1855	560	20
Creep (compression, $2–500 \times 10^{-5}$ s^{-1}, $n = 5$)	TiC_{1-x}	~2000	>560	20
Creep (compression and bending, $n = 2.7$)	TiC_{1-x}	1400–1700	380	46
Creep (compression and bending, $n = 3.5$)	TiC_{1-x}	1700–2000	650	46
Creep (bending, 5–17 MPa, $n = 1$)	$TiC_{0.95}$	2000–2300	425 ± 20	19
Creep (bending, 17–30 MPa, $n = 3$–4)	$TiC_{0.95}$	2300–2600	600 ± 30	19
Creep (bending, 5–12 MPa, $n = 1$)	$TiC_{0.94}$	2300–2600	625 ± 30	18
Creep (tension, 48–55 MPa)	$TiC_{0.96}$	1640–1700	542	47
Creep (tension, 48–55 MPa)	$TiC_{0.96}$	1730–1810	730	47
Creep (extrapolation of calculated data)	$TiC_{1.0}$	910–1180	160	48
Creep (extrapolation of calculated data)	$TiC_{1.0}$	1230–2000	520	48
Creep (bending, 3–10 MPa, $n = 1$)	TiC–C[g]	2400–2800	$590–680 \pm 30$	49
Creep (bending, 3–10 MPa, $n = 1$)	TiC–C[h]	2400–2800	$545–660 \pm 30$	49

[a] Sintered body after volume deformation.
[b] After surface cold-hardening.
[c] Pressureless sintered powders.
[d] Grain growth during solid-state hot-pressing of titanium carbide with metal titanium.
[e] Grain growth during liquid-phase sintering of titanium carbide with metal titanium.
[f] Sintered body.
[g] Added 6–28 vol% carbon black.
[h] Added 6–28 vol% flake graphite.

Table 4
Values of apparent activation energy Q for densification processes during hot-pressing of transition metal carbides

Composition	Temperature range (°C)	Applied pressure (MPa)	Relative density (γ)	Activation energy Q (kJ mol^{-1})	Reference
$TiC_{0.63–0.94}$[a]	1200–1600	7–35	0.84–1.0	117 ± 5–10%	39
$TiC_{0.96}$	2100–2300	16	~0.94	140 ± 5–10%	6
$TiC_{0.93}$	1300–1900	25–120	0.85–0.95	180–315	50
$TiC_{0.95}$	2200–2500	8–30	0.94–0.96	$285–335 \pm 5$%	7
$TiC_{0.95}$[b]	2000–2600	5–25	0.75–1.0	380	22
$TiC_{0.94}$	2100–2700	5–13	0.65–0.97	510	22
80 vol.% TiC–20 vol.% C	2200–2400	8–16	0.64–0.98	270 ± 30	Present work
$ZrC_{0.96}$	1700–2400	40	0.75–0.98	170	51
$ZrC_{1.0}$	2200–2400	16	~0.91	190 ± 5–10%	6
$ZrC_{0.92}$	2200–2600	10–30	0.94–0.96	$270–285 \pm 5$%	7
$HfC_{1.0}$	2500–2700	16	~0.92	215 ± 5–10%	6
$VC_{0.85}$	2000–2400	10–30	0.94–0.96	$160–180 \pm 5$%	7
$NbC_{0.74}$[c]	1460–1660	48–54	<0.93	240 ± 10	52
$NbC_{0.74}$[c]	1630–1830	64	0.93–0.99	470	52
$NbC_{0.99}$	2200–2400	16	~0.89	360 ± 5–10%	6
$TaC_{1.0}$	2600–2800	16	~0.91	405 ± 5–10%	6

[a] Reactive solid-state hot-pressing of titanium carbide with metal titanium.
[b] Iron contaminated: 0.2 wt.%.
[c] Hot isostatically pressed.

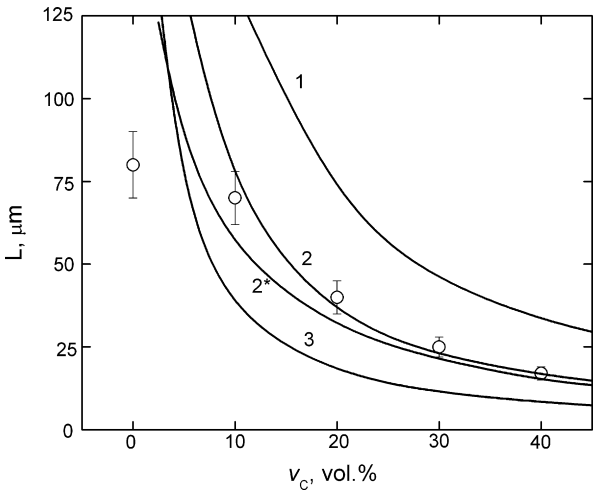

Fig. 10. Dependencies of the average matrix grain size L for the TiC–C hot-pressed compositions on the volume fraction of graphite inclusions (experimental dots). Calculated curves according to Eq. (18) for different values of r: (1) 10 μm; (2) 5 μm; (3) 2.5 μm and Eq. (19) for $\bar{r}$: (2^*) 5 μm.

lation sliding and the fragmentation of particles play the most important role for the densification process. Practically, these processes finish during the heating before the isothermal soaking or at the beginning of it as it is shown, in particular, by the non-linear character of dependency $\Delta X_3(\gamma) - \tau$ during the initial stage (see Fig. 8b), where the value $n < 3$. Probably, interface and boundary processes, such as grain slipping, angular rotation and others contribute in certain ways to the deformation of porous composition during the subsequent stages of hot-pressing. The proof of this tendency could be the lower value of Q obtained experimentally in this work, but also the manifestation of superplasticity revealed in the TiC–C system, where it was observed the anomalous increase of creep rate for the quasi-eutectic compositions[49].

The presence of low-modulus graphite inclusions retards the recrystallization of titanium carbide matrix. It was found that the observed microstructure of the hot-pressed TiC–C HMC is well described by the formula, which is analogous to the classical Zener pinning equation for stable grain size[53]:

$$L = \frac{4}{3}\frac{r}{(v_C/100)} \tag{18}$$

where L is the average matrix (titanium carbide) grain size and r is the nominal drag radius of pinning force. This fact is evidenced by the plot of L versus v_C, where obtained experimental data on the TiC–C HMC with different graphite content (Fig. 10, dots) are compared with results calculated accordingly to Eq. (18) (Fig. 10, curves) for the values of r equal to 2.5, 5 and 10 μm. In the hot-pressed HMC, the most significant pinning force is exerted by graphite particles,[3] but another factor that inhibits grain boundary motion is the influence of pores. Therefore, taking into account this factor, the expression for porosity: $p = 1 - \gamma$ and general relation $v_{TiC} + v_C = 100$ Eq. (18) should be transformed as

$$L = \frac{4}{3}\frac{\bar{r}}{(1 - (v_{TiC}/100)\gamma)} \tag{19}$$

which includes $\bar{r}$ that merges both inhibiting factors: graphite particles and pores, and corresponds approximately to the linear size of "general drag" $2\bar{r} = 10$ μm.

Graphite inclusions result in the conservation of a widely developed grain boundary network, which plays the role of quasi-amorphous sinks or shorter diffusion paths (circuits) for point defects, mostly vacancies, from sources to the external boundary of compacts. Obviously, this is the most important distinction between carbide–graphite HMC and single phase carbide materials, which leads to the extremely different viscosity—time relations for these materials during the hot-pressing (see Fig. 4). The collective recrystallization of single phase materials accompanied by the significant grain growth causes viscosity of porous body to rise gradually while porosity is decreasing during the hot-pressing (sintering) process. Samsonov and Kovalchenko[54] made an attempt to take it into account by the introduction of special modification of Eq. (4):

$$\eta = \eta'(1 + b\tau) \tag{20}$$

where b is a constant coefficient for given temperature corresponding to grain growth rate. Probably, it is possible to find out the direct links between b and grain growth kinetics constants, but unfortunately, there are no experimental data in literature to compare these links for different types of materials.

3.5. Densification mechanism

Hot-pressing and sintering of powder refractory compound compositions relate to the diffusion-controlled processes, which are determined in binary systems not only by individual partial coefficients of self-diffusion for components, but also by an effective coefficient, the so called chemical interdiffusion coefficient[16]. While healing macrodefects, e.g. pores, there is a strong possibility of dehomogenization in carbide phase due to considerable difference (10^2–10^4 times) in metal and carbon atoms mobilities[32–34]. The presence of great amounts of excess carbon obviously changes the concentrations of point and linear defects in carbide matrix phase compared with those for quasi- or hypo-stoichiometric carbides, therefore the densification of carbide–graphite HMC is developing in different way. At the same time with the sintering of carbide phase the noticeable rearrangement of graphite phase takes place during the treatment. It is realized en route to the deeper ordering of atomic structure, which brings about the reduction of interlayer spacing for graphite from $d = 0.339$ nm up to $d = 0.335$ nm. This variation of volume corresponds to 1.2% that is commensurate with the residual porosity of material in the final stage of hot-pressing. Difference in electron structure of carbide and graphite cause considerable discrepancy in self-diffusion coefficients of carbon in these phases that leads to some difficulties in the formation of interphase contact between carbide and graphite micrograins in the initial stage, but also in its extension during consequent stages of sintering or hot-pressing. At high temperatures besides the solid-state diffusion mechanisms mass transport in porous carbide–graphite compositions is realized by vaporization–condensation reactions[55]. Graphite particles possess flakes form, so the greater part of their surface relates to

basal planes (0 0 l), which are characterized by covalent bonds with high grade of directivity and enrichment; such characteristics make the surface of graphite particles relatively inert for contact interaction. Metal diffusion coefficients in the normal direction to the basal plane approximately twice less than in the parallel direction, and the value of activation energy of diffusion in normal direction is 10% higher[56]. The high anisotropy of the physical properties of graphite causes the thermal expansion in perpendicular direction to the basal planes to be 200 times higher than in parallel, so it is not unexpected that the compressibility of graphite microcrystals in the perpendicular direction to the basal planes is 10^4–10^5 times greater. In cooperative effect together with the reduction of interlayer spacing and the preferential orientation of the graphite inclusions[57] during high-temperature hot-pressing these phenomena lead to the perturbation of continuity and high grade of defectiveness for the carbide–graphite interface and, additionally, brings about the reduction of HMC relative density with increase of carbon volume content[3].

After the qualitative consideration of the densification kinetics, it is necessary to pass on to the quantitative characteristics of this process, which are obtained in the present work. It is rather clear that the first main constant, exponent n, which value equalled 3, identifies the TiC–C HMC hot-pressing process as deformation realized by intraparticle (lattice dislocation) mechanism[15] in carbide micrograins. But it is quite difficult to find an appropriate explanation for the apparent activation energy Q, which value of $270 \pm 30\,\mathrm{kJ\,mol^{-1}}$ is far from lattice self-diffusion constants for both titanium[33] and carbon[34,35]. Unfortunately, the present work is a pioneer in hot-pressing kinetics of the MeC—C HMC, so there is no chance to compare the obtained value with those in analogous systems, but, nevertheless, there are some papers on the hot-pressing of TiC and ZrC, which submit close values for activation energy Q (see Table 4). The values close to the energy activation for dislocation slip mechanism,[58] which is proposed to be about $200\,\mathrm{kJ\,mol^{-1}}$, were claimed also for the apparent activation energy of titanium carbide recrystallization[40–42]. Undoubtedly, the kinetics data are linked to two main high-temperature processes, such as densification and grain growth, so they should be considered jointly. However, the interpretation of Q in the case of hot-pressing and recrystallization of refractory compound compositions requires certain caution. Both of these processes often involve several mechanisms of mass transport, which may operate whether independently as parallel mechanisms, so, e.g. in the case of creep consideration:$\dot{\varepsilon} = \sum_{n=i}^{n=1} \dot{\varepsilon}_i$, or sequentially, as serial mechanisms: $\dot{\varepsilon} = 1/\sum_{n=i}^{n=1}(1/\dot{\varepsilon}_i)$. There is simpler situation with the latter one, because in this case the slower process determines entirely the value of Q. Any diffusion mechanism includes two sequential processes, such as the formation/annihilation of point defects and motion of them through volume, along the grain boundaries or via dislocation core.

The experimentally obtained value of Q will have an unequivocal meaning only if the conditions are controlled by the same diffusion mechanism. Otherwise, it will be difficult to interpret Q values, if you do not use special description for diffusion process, like, e.g. in the case of power-law-creep operated by climb-plus-glide mechanism[16]. This mechanism can also occur in the TiC–C HMC at high temperatures, when carbon diffusion controls the non-conservative dislocation motion under loading and the transport of matter occurs by lattice diffusion as well as dislocation core diffusion. Different mechanisms may contribute to the overall diffusive transport more or less significantly in different ranges of temperatures and stresses, so it is necessary to use the value of effective diffusion coefficient[16]:

$$D = D_1 f_1 + D_2 f_2 \tag{21}$$

where D_1, D_2 are, respectively, the lattice and dislocation core diffusion coefficients and f_1, f_2 respectively, the fractions of atom sites associated with each type of diffusion.

The most acceptable way to explain the value of Q obtained in the present work is to propose that diffusion along the grain boundaries predominates as a mechanism of mass transport while the TiC–C compositions are hot-pressed in the studied range of temperatures and applied pressures. Though, Frost and Ashby[16] proposed for the transition metal carbides ZrC and TiC higher values for both boundary and core diffusion activation energy, these values are in good agreement with data submitted for short circuit diffusion in TiC_{1-x} by Adelsberg and Cadoff,[36] Vansant and Phelps[37] and Sura and Kohlstedt[50] (see Tables 3–4). Therefore, it can be concluded that during hot-pressing the densification of the TiC–C compositions is controlled by grain-boundary or dislocation core diffusion of carbon and/or titanium in the carbide phase.

Obviously, it is necessary to carry out further investigation to clarify that point, because, the models applied in this work, unfortunately, do not allow to identify the individual mechanisms and determine their contributions to the general process of densification. Another disadvantage of the obtained mathematical description is that when analyzing creep process during hot-pressing, it does not take into account the elasticity modulus dependency on temperature. Only application of the similar function helped to select the different mechanisms in creep process for some high-temperature materials[59].

Finally, it is necessary to state that the next step of the refractory compound—graphite HMC hot-pressing exploration should be the superposed analysis of microstructure kinetics for porosity and grain growth of the materials while thermal and pressure loading. It is not only interesting to understand high-temperature physical and chemical effects better, but also is very useful for manufacturing practice. The application of sintered hard alloys (cermets) allows utilization of the hardness of carbides, nitrides, borides and similar compounds for engineering purposes, but utilization of their excellent high-temperature properties would be possible in HMC. Therefore, the development of hot-pressing technique of this class of ceramics, as the most successful method of its manufacturing, is of great practical importance.

4. Conclusions

The present work was, essentially, a study of densification and crystallization behavior during hot-pressing of hetero-modulus ceramic–ceramic composite materials (HMC), which present

the combination of ceramic matrix with high Young's modulus and the inclusions of a dispersed phase with low Young's modulus. The following conclusions concerning 60–100 vol% TiC–0–40 vol% C (graphite) powder compositions, which were hot-pressed at 2200–2400 °C and applied pressures of 8–16 MPa can be drawn:

(1) The developed relation from the general theory of bulk-viscous flow as well as Kovalchenko's equation for the evolution of relative density for non-uniform deformation of porous body, incorporating different stages of creep, can be successfully used for the interpretation of densification kinetics. Due to the application of these functional dependencies it became possible to determine the activation energy Q and the power-law exponent constant n of the hot-pressing process, which values were equal $270 \pm 30\,\mathrm{kJ\,mol^{-1}}$ and 3 ± 0.3, respectively.
(2) The presence of low-modulus graphite inclusions retards the recrystallization of titanium carbide matrix. The increase of graphite content from 10 to 40 vol% caused the reduction of mean TiC matrix grain size on 3–4 times. The saturated by carbon TiC phase in HMC is characterized by lower values of lattice parameter ($a = 0.4326$ nm) and microhardness (HV = 24 GPa) compared with those for quasi-stoichiometric TiC_{1-x}. The microstructure of the hot-pressed TiC–C composites with different graphite content is well described by the classical Zener pinning equation for stable grain size. The reduction of the TiC–C compositions density observed with increase of graphite content is explained by the cooperative effect of several factors, such as the reduction of graphite interlayer spacing from $d = 0.339$ nm up to $d = 0.335$ nm during high-temperature hot-pressing, the diffusion difficulties for metal atoms in the normal direction to the basal planes (0 0 l), and the high value of anisotropy of thermal expansion and compressibility for graphite microcrystals.
(3) The kinetics analysis of the hot-pressing process for the TiC–C HMC shows that the densification is controlled by power-law creep process characterized by $\dot{\varepsilon} \propto \sigma^3$. Though this mechanism of thermally activated glide-controlled creep is often observed during the ceramics processing, there are some particularities in the densification and recrystallization behavior, which are inherent, probably, namely to the HMC, because of their specific physico-chemical properties and microstructure. The most likely mechanism of mass transport in the TiC–C HMC in the studied range of temperatures and applied pressures is grain-boundary or dislocation core diffusion of carbon and/or titanium in the carbide phase.

Acknowledgements

The authors wish to thank Prof. A.R. Beketov, Ural State Technical University, Russia and Prof. G.M. Romantsev, Russian State Professional and Pedagogical University for providing the necessary technological and research facilities. One of the authors, I.L. Shabalin, would like to express his gratitude to Prof. D.K. Ross and Dr. D.J. Bull for support and help in the preparation of this work for publishing.

References

1. Hasselman, D. P. H., Becher, P. F. and Mazdiyasni, K. S., Analysis of the resistance of high-E, low-E brittle composites to failure by thermal shock. *Z. Werkstofftech.*, 1980, **11**(3), 82–92.
2. Zhukov, Yu. N., Cherepanov, A. V., Beketov, A. R. and Shabalin, I. L., Inspection of the nonuniformity of a ceramic compact for machining by hardness measurement. *Sov. Powder Metall. Met. Ceram.*, 1991, **30**(4), 349–351.
3. Shabalin, I. L., Beketov, A. R., Gorinskii, S. G., Podkovyrkin, M. I. and Fedorenko, O. V., Study of strength characteristics of titanium carbide–silicon carbide–carbon hot-pressed materials. In *Alloys of Refractory and Rare Metals for High-Temperature Application. Proceedings of the All-USSR Conference on Physico-Chemical Principles of Development for Heat-Resisting Metal Materials*, ed. E. M. Savitskii, 1984, pp. 186–189.
4. Araki, M., Sasaki, M., Kim, S., Suzuki, S., Nakamura, K. and Akiba, M., Thermal response experiments of SiC/C and TiC/C functionally gradient materials as plasma facing materials for fusion application. *J. Nucl. Mater.*, 1994, **212–215**, 1329–1334.
5. Ramqvist, L., Hot pressing of metallic carbides. *Powder Metall.*, 1966, **9**(17), 26–46.
6. Samsonov, G. V., Kovalchenko, M. S., Petrykina, R. Ya. and Naumenko, V. Ya., Hot pressing of the transition metals and their carbides in their homogeneity regions. *Sov. Powder Metall. Met. Ceram.*, 1970, **9**(9), 713–716.
7. Spivak, I. I. and Klimenko, V. V., Densification kinetics in the hot pressing and recrystallization of carbides. *Sov. Powder Metall. Met. Ceram.*, 1973, **12**(11), 883–887.
8. Taylor, N., Dunand, D. C. and Mortensen, A., Initial stage hot pressing of monosized Ti and 90% Ti–10% TiC powders. *Acta Metall. Mater.*, 1993, **41**(3), 955–965.
9. Ting, C.-J. and Lu, H.-Y., Hot-pressing of magnesium aluminate spinel. I. Kinetics and densification mechanism. *Acta Mater.*, 1999, **47**(3), 817–830.
10. Hays, C. and Kendall, E. G., Improved metallography for TiC and TiC–C alloys. *J. Am. Ceram. Soc.*, 1965, **48**(1), 50–51.
11. Skorokhod, V. V., *Rheological Principles of the Theory of Sintering*. Naukova Dumka, Kiev, 1972, pp. 21–23.
12. Kovalchenko, M. S., A study of hot-pressing processing of powders. In *Metal–Ceramic Materials and Products*. Yerevan Polytechnic Institute, Yerevan, 1969, pp. 91–94.
13. Landau, L. D. and Lifschitz, E. M., *Mechanics of Continuum Media*. Butterworth–Hernemann, New York, 1976, pp. 45–46.
14. Wang, J. N. and Niech, T. G., Role of Peierls stress in power law dislocation creep. *Mater. Sci. Eng A Struct. Mater., Prop. Microstruct. Process.*, 1995, **A202**(1–2), 52–56.
15. Pampuch, R., Mechanisms of hot pressing of magnesium oxide powders. *Ceramurgia Intern.*, 1979, **5**(2), 76–83.
16. Frost, H. J. and Ashby, M. F., *Deformation–Mechanism Maps. The Plasticity and Creep of Metals and Ceramics*. Pergamon Press, Oxford, 1982, pp. 11–83.
17. Williams, W., Influence of temperature, strain rate, surface condition and composition on the plasticity of transition-metal carbide crystals. *J. Appl. Phys.*, 1964, **35**(4), 1329–1338.
18. Spivak, I. I. and Klimenko, V. V., Study of diffusion effects on interstitial phases. *Phys. Met. Metallogr.*, 1971, **32**(2), 87–92.
19. Spivak, I. I., Andrievskii, R. A., Rystsov, V. N. and Klimenko, V. V., Creep of titanium monocarbide in its homogeneity range. *Sov. Powder Metall. Met. Ceram.*, 1974, **13**(7), 574–578.
20. Tsurekawa, S., Matsubara, S., Kurishita, H. and Yoshinaga, H., Steady state deformation mechanism in titanium carbide. *Mater. Trans. JIM*, 1991, **32**(9), 821–828.
21. Kovalchenko, M. S., Steady-state and transient creep stages in the sintering of porous materials. *Sov. Powder Metall. Met. Ceram.*, 1971, **10**(10), 795–801.
22. Kovalchenko, M. S. and Ochkas, L. F., Creep in the hot pressing of titanium carbide powder. *Sov. Powder Metall. Met. Ceram.*, 1973, **12**(1), 23–31.

23. Kovalchenko, M. S. and Ochkas, L. F., Creep during hot pressing of zirconium carbide powder. In *Proceedings of the All-Union Scientific and Technological Conference on Metal-Ceramic Materials and Products*. Yerevan Polytechnic Institute, Yerevan, 1973, pp. 139–143.
24. Kovalchenko, M. S., Creep in the hot pressing of powders of titanium nitride, molybdenum disilicide and zirconium and chromium diborides. *Sov. Powder Metall. Met. Ceram.*, 1973, **12**(4), 272–276.
25. Kovalchenko, M. S. and Mai, M. M., Creep in the hot pressing of titanium diboride powder. *Sov. Powder Metall. Met. Ceram.*, 1973, **12**(8), 622–625.
26. Kovalchenko, M. S., Bogomol, I. V. and Serebryakova, T. I., Kinetics of the hot pressing of titanium and tungsten carbide alloys cemented with niobium. *Sov. Powder Metall. Met. Ceram.*, 1972, **11**(6), 441–445.
27. Kovalchenko, M. S. and Sereda, N. N., A study of densification kinetics during hot pressing, structure and properties in hard alloy based on titanium carbide. In *Hot Pressing*, *Vol. 2*, ed. M. S. Kovalchenko. Institute for Problems of Materials Science, Ukranian SSR Academy of Science, Kiev, 1974, pp. 114–118.
28. Denisenko, E. T. and Mai, V. K., Densification kinetics in the hot pressing of metal powders. *Sov. Powder Metall. Met. Ceram.*, 1968, **7**(11), 858–862.
29. Kovalchenko, M. S., Ogorodnikov, V. V., Rogovoi, Yu. I. and Kraynii, A. G., Calculation of vacancies formation and motion energies in refractory compounds. In *Radiation Damage of Refractory Compounds*. Atomizdat, Moscow, 1979, pp. 160–165.
30. Turchanin, A. G., Calculation of carbon vacancy formation energy for transition metal carbides. *Zhurnal Fizicheskoi Khimii*, 1980, **54**(11), 2962–2964.
31. Kohlstedt, D. L. and Williams, W. S., Investigation of the charge distribution in titanium carbide using electromigration. *Phys. Rev. B Condens. Matter*, 1971, **3**(2), 293–305.
32. Fryt, E. M., Defect mobility in TiC_{1-x} at high temperatures. *Solid State Ionics*, 1997, **101–103**(1), 437–443.
33. Sarian, S., Diffusion of Ti-44 in TiC_x. *J. Appl. Phys.*, 1969, **40**(9), 3515–3520.
34. Sarian, S., Diffusion of carbon in TiC. *J. Appl. Phys.*, 1968, **39**(7), 3305–3310.
35. Kohlstedt, D. L., Williams, W. S. and Woodhouse, J. B., Chemical diffusion in titanium carbide crystals. *J. Appl. Phys.*, 1970, **41**(11), 4476–4484.
36. Adelsberg, L. M. and Cadoff, L. H., Reactions of liquid titanium and hafnium with carbon. *Trans. Met. Soc. AIME*, 1967, **239**(6), 933–935.
37. Vansant, C. A. and Phelps Jr., W. C., Carbide formation from beta-titanium and graphite. *Trans. ASM*, 1966, **59**(1), 105–112.
38. Samsonov, G. V. and Kushtalova, I. P., Deformation and recrystallization of refractory compounds. *Izv. Akad. Nauk SSSR Neorg. Mater.*, 1973, **9**(1), 46–47.
39. Bozhko, S. A. and Samsonov, G. V., Mechanism of collective recrystallization in titanium carbide. *Sov. Powder Metall. Met. Ceram.*, 1970, **9**(2), 127–131.
40. Samsonov, G. V. and Bozhko, S. A., Recrystallization during the sintering of niobium and titanium carbide powders. *Sov. Powder Metall. Met. Ceram.*, 1969, **8**(7), 542–546.
41. Quinn, C. J. and Kohlstedt, D. L., Reactive processing of titanium carbide with titanium. 2. Solid-state hot pressing. *J. Mater. Sci.*, 1984, **19**(4), 1242–1250.
42. Kushtalova, I. P., Investigation of the sintering of loosely poured titanium carbide and niobium carbide powders. *Sov. Powder Metall. Met. Ceram.*, 1967, **6**(8), 604–605.
43. Quinn, C. J. and Kohlstedt, D. L., Reactive processing of titanium carbide with titanium. 1. Liquid-phase sintering. *J. Mater. Sci.*, 1984, **19**(4), 1229–1241.
44. Kurishita, H., Nakajima, K. and Yoshiga, H., The high temperature deformation mechanism in titanium carbide single crystals. *Mater. Sci. Eng.*, 1982, **54**(2), 177–190.
45. Sura, V. M. and Kohlstedt, D. L., Inelastic deformation of (Ti, V) C alloys. 2. Load relaxation studies. *J. Mater. Sci.*, 1986, **21**(7), 2356–2364.
46. Chermant, J.-L., Leclerc, G. and Mordike, B. L., Deformation of titanium carbide at high temperatures. *Z. Metallkd.*, 1980, **71**(7), 465–469.
47. Keihn, F. and Kebler, R., High-temperature ductility of large-grained TiC. *J. Less-Common Met.*, 1964, **6**(6), 484–485.
48. Munoz, J. D., Arizmendi, A., Mendoza-Allende, A. and Montemayor-Aldrete, J. A., High temperature activation energy for plastic deformation of titanium carbide single crystals as a function of the C:Ti atom ratio. *J. Mater. Sci.*, 1997, **32**(12), 3189–3193.
49. Spivak, I. I., Andrievskii, R. A. and Klimenko, V. V., Creep of two-phase titanium carbide alloys. *Sov. Powder Metall. Met. Ceram.*, 1974, **13**(3), 93–97.
50. Sura, V. M. and Kohlstedt, D. L., Inelastic deformation of (Ti, V) C alloys. 1. Hot-pressing kinetics. *J. Mater. Sci.*, 1986, **21**(7), 2347–2355.
51. Barnier, P., Brodhag, C. and Thevenot, F., Hot-pressing kinetics of zirconium carbide. *J. Mater. Sci.*, 1986, **21**(7), 2547–2552.
52. Nixon, R. D., Chevacharoenkul, S. and Davis, R. F., Steady-state behavior of hot isostatically pressed niobium carbide. *Mater. Res. Bull.*, 1987, **22**(9), 1233–1240.
53. Helle, A. S., Easterling, K. E. and Ashby, M. F., Hot-isostatic pressing diagrams: new developments. *Acta Metall.*, 1985, **33**(12), 2163–2174.
54. Samsonov, G. V. and Kovalchenko, M. S., *Hot pressing*. Gostekhizdat UkrSSR, Kiev, 1962, pp. 40–42.
55. Gorinskii, S. G., Beketov, A. R., Shabalin, I. L., Podkovyrkin, M. I. and Kokorin, A. F., Electrical resistivity of hot-pressed TiC–SiC–C composite materials. *Sov. Powder Metall. Met. Ceram.*, 1982, **21**(11), 867–871.
56. Weisweller, W. and Alavi, M., Anisotrope diffusions—kinetik von metallen und carbiden in pyrographit. *Ber. Dtsch. Keram. Ges.*, 1976, **53**(6), 179–183.
57. Pakholkov, V. V., Gorinskii, S. G., Beketov, A. R., Shabalin, I. L. and Ragozin, S. V., Texture of hot-pressed vanadium carbide–carbon materials. *Sov. Powder Metall. Met. Ceram.*, 1986, **25**(8), 661–663.
58. Kovalchenko, M. S., Dzhemelinskii, V. V., Skuratovskii, V. N., Tkachenko, Yu. G., Yurchenko, D. Z. and Alekseev, V. I., Microhardness of some carbides at various temperatures. *Sov. Powder Metall. Met. Ceram.*, 1971, **10**(8), 665–668.
59. Robinson, S. L. and Sherby, O. D., Mechanical behaviour of polycrystalline tungsten at elevated temperature. *Acta Metall.*, 1969, **17**(2), 109–125.